Miner Petrol (2011) 103:149–167
DOI 10.1007/s00710-011-0165-7

ORIGINAL PAPER

Magma mixing/mingling in the Eocene Horoz (Nigde) granitoids, Central southern Turkey: evidence from mafic microgranular enclaves

Kerim Kocak · Veysel Zedef · Gursel Kansun

Received: 6 December 2010 / Accepted: 15 July 2011 / Published online: 30 July 2011
© Springer-Verlag 2011

Abstract Mafic microgranular enclaves (MMEs) are widespread in the Horoz pluton with granodiorite and granite units. Rounded to elliptical MMEs have variable size (from a few centimetres up to metres) and are generally fine-grained with typical magmatic textures. The plagioclase compositions of the MMEs range from An_{18}–An_{64} in the cores to An_{17}–An_{29} in the rims, while that of the host rocks varies from An_{17} to An_{55} in the cores to An_{07} to An_{33} in the rims. The biotite is mostly eastonitic, and the calcic-amphibole is magnesio-hornblende and edenite. Oxygen fugacity estimates from both groups' biotites suggest that the Horoz magma possibly crystallised at fO_2 conditions above the nickel–nickel oxide (NNO) buffer. The significance of magma mixing in their genesis is highlighted by various petrographic and mineralogical characteristics such as resorption surfaces in plagioclases and amphibole; quartz ocelli rimmed by biotite and amphibole; sieve and boxy cellular textures, and sharp zoning discontinuities in plagioclase. The importance of magma mixing is also evident in the amphiboles of the host rocks, which are slightly richer in Si, Fe^{3+} and Mg in comparison with the amphiboles of MMEs. However, the compositional similarity of the plagioclase and biotite phenocrysts from MMEs and their host rocks suggests that the MMEs were predominantly equilibrated with their hosts. Evidence from petrography and mineral chemistry suggests that the adakitic Horoz MMEs could be developed from a mantle-derived, water-rich magma (>3 mass%) affected by a mixing of felsic melt at P >2.3 kbar, T >730°C.

Editorial handling: R. Milke

K. Kocak (✉) · G. Kansun
Department of Geological Engineering, Selcuk University,
Konya 42075, Turkey
e-mail: kkocak@selcuk.edu.tr

V. Zedef
Department of Mining Engineering, Selcuk University,
Konya 42075, Turkey

Introduction

Mafic microgranular enclaves (MME) are widespread in intermediate and felsic granitoids. The characterisation, genesis and evolution of MMEs have been widely discussed by several authors (e.g., Didier 1973; Hibbard 1981; Vernon 1983; Didier and Barbarin 1991). The three main theories for the petrogenesis of microgranular enclaves are as follows: (1) they form by settling of early crystals from the host magma or by fragmentation of early solidified wall-rock facies closely related to the host magma cognate fragments of cumulate minerals from a mafic magma (e.g., Noyes et al. 1983; Chappell et al. 1987; Dahlquist 2002; Ilbeyli and Pearce 2005); (2) they are fragments of recrystallised, refractory metamorphic rocks and fragments of melt residues from the granite source (e.g., Chappell et al. 1987; Chappel and White 1992; White et al. 1999); or (3) they are globules of more mafic magma, generally hybrid magma, comingled with a more felsic host magma (e.g., Vernon 1984; Dorais et al. 1990; Blundy and Sparks 1992; Wiebe et al. 1997; Kadioglu and Gulec 1999; Perugini et al. 2003; Barbarin 2005; Kocak 2006; Feeley et al. 2008; Kaygusuz and Aydıncakır 2009). The hybridism model, in particular has been well documented by many geologists (e.g., Frost and Mahood 1987; Didier and Barbarin 1991; Michael 1991; Blundy and Sparks 1992; Silva et al. 2000; Barbarin 2005) and has been applied in studies of granites worldwide.

Previous studies of the Horoz Granodiorite have reported that magma mingling had occurred (e.g., Çevikbaş et al.

1995; Kocak 2000; Kadioglu and Dilek 2009), but the mineral chemistry of the enclaves has not been investigated. The aim of this study is to present the mineral chemistry of the Horoz granitoid and to investigate the chemical and physical interaction between felsic and mafic magmas.

Geological setting

Turkey is situated on an E–W-trending fragment of the Alpine–Himalayan orogenic belt. This fragment contains a few continental blocks divided by suture zones developed by the closure of the different branches of the Neo-Tethyan Ocean during the late Cretaceous–Eocene (Sengor and Yilmaz 1981) (Fig. 1). Two subduction zones with opposite vergences are proposed to have created a double granitic arc in the north (Central Anatolian Crystalline Complex, CACC, Kirsehir Block of Gorur et al. 1984) and in the south (Taurides).

The granitic intrusions along the northern edge of the Taurides may have been developed in relation to the evolution of the Neo-Tethyan "Inner Tauride Ocean" (Gorur et al. 1984; Dilek et al. 1999), which began to form as early as the Jurassic between CACC to the east and the Taurides to the west. The ocean was consumed by an intra-oceanic subduction northwards (Gorur et al. 1998) along the Inner-Tauride Suture Zone (ITSZ), which is defined by discontinuous exposures of the Cenomanian–Turonian suprasubduction zone ophiolites (i.e., Alihoca, Aladag) and melanges that occurred by the latest Cretaceous (Clark and Robertson 2002). The measured ages of the different parts of the ophiolites along the Tauride belt show that the subduction-related magmatic activity was initiated in the Turonian and continued until the end of Maastrichtian prior to their emplacement onto the Tauride platform (Parlak et al. 2010).

The study area is situated at the eastern part of the Bolkar Mountains (Nigde, Central Southern Turkey, Fig. 1), adjacent to ITSZ, between two continental blocks, the Taurides and the CACC. The Bolkar Mountain units, the oldest in the area, make up the heights of the Bolkar Mountains due to an anticline they form. The units include variably metamorphosed Upper Permian-Upper Triassic platform carbonates with siliciclastic intercalations, which

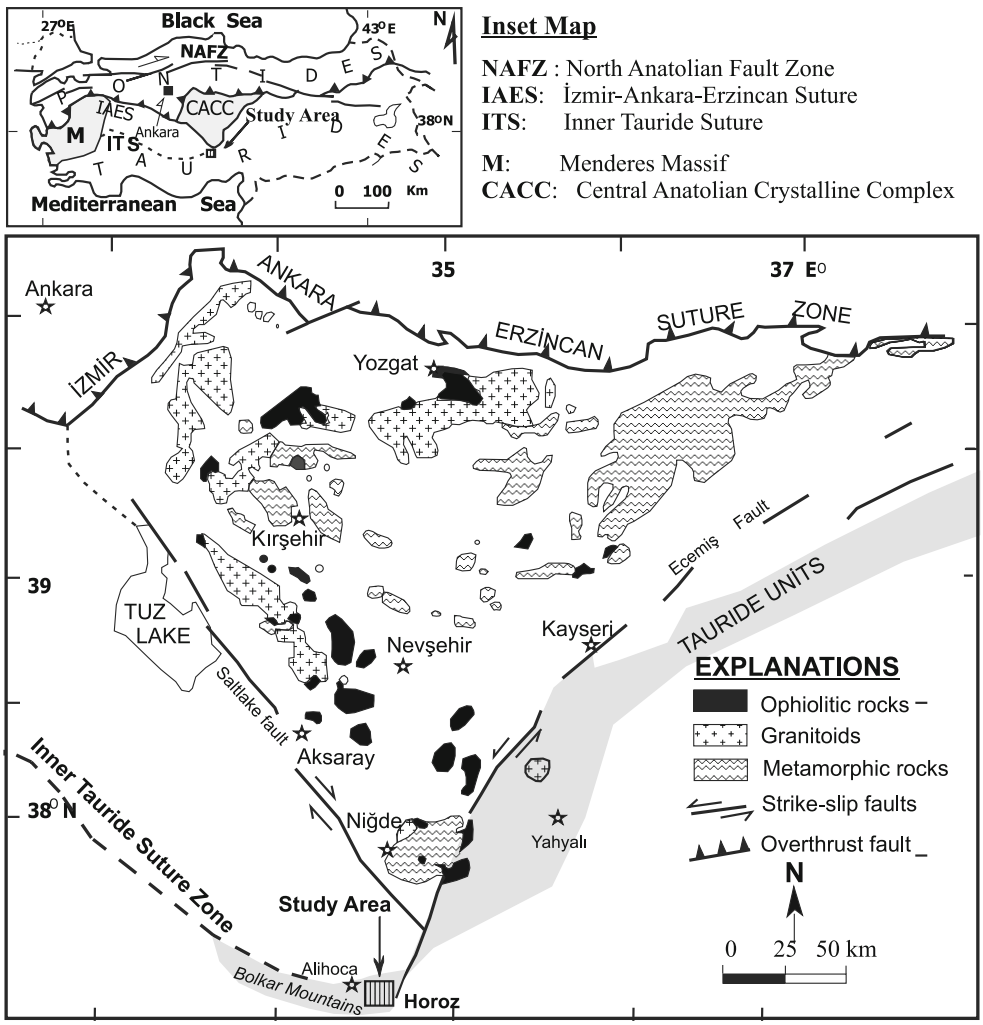

Fig. 1 Generalised geological sketch map of the main lithologic units of the Central Anatolian Crystalline Complex (CACC, after Bingol 1974)

were intruded by an ENE–WSW-trending, sill-like pluton (the Horoz granitoid, Fig. 2), along with the development of some economic skarn mineralisation. The Horoz granitoid is of shallow-seated intrusions and is cropped out in the so-called Horoz Valley. The pluton was intruded by later tonalitic/dioritic dikes (Fig. 3a) with a sharp contact that has a thickness ranging from 10 cm to 10 m and may continue locally for 100–250 m along-strike (Çalapkulu 1980). Aplite veins may cut the enclave mingled with plastic granitoid magma. The granitoid was overlaid by Upper Cretaceous Alihoca ophiolites, which are composed of the following: (a) medium-grained basic and ultrabasic rocks; (b) volcanosedimentary rocks, observed as klippe at the high hill of the Bolkar Mountains; (c) diabases, spilite and volcanic rocks; and d) albite-epidote-actinolite-glaucophane bearing schists. The ophiolite is dismembered as thrust sheets and blocks within an extensive ophiolitic mélange and is overlain by a U. Maestrichtian-L. Paleocene Kalkankaya formation, including conglomerates, limestone with rudists and argillecous limestone. The granitoid was covered with nonconformity by Oligocene terrace deposits at the southern part of the valley. Accordingly, the granitoid was suggested to be emplaced between the Lower Paleocene and Lower Eocene (Çalapkulu 1980). The age of the Horoz pluton was recently determined

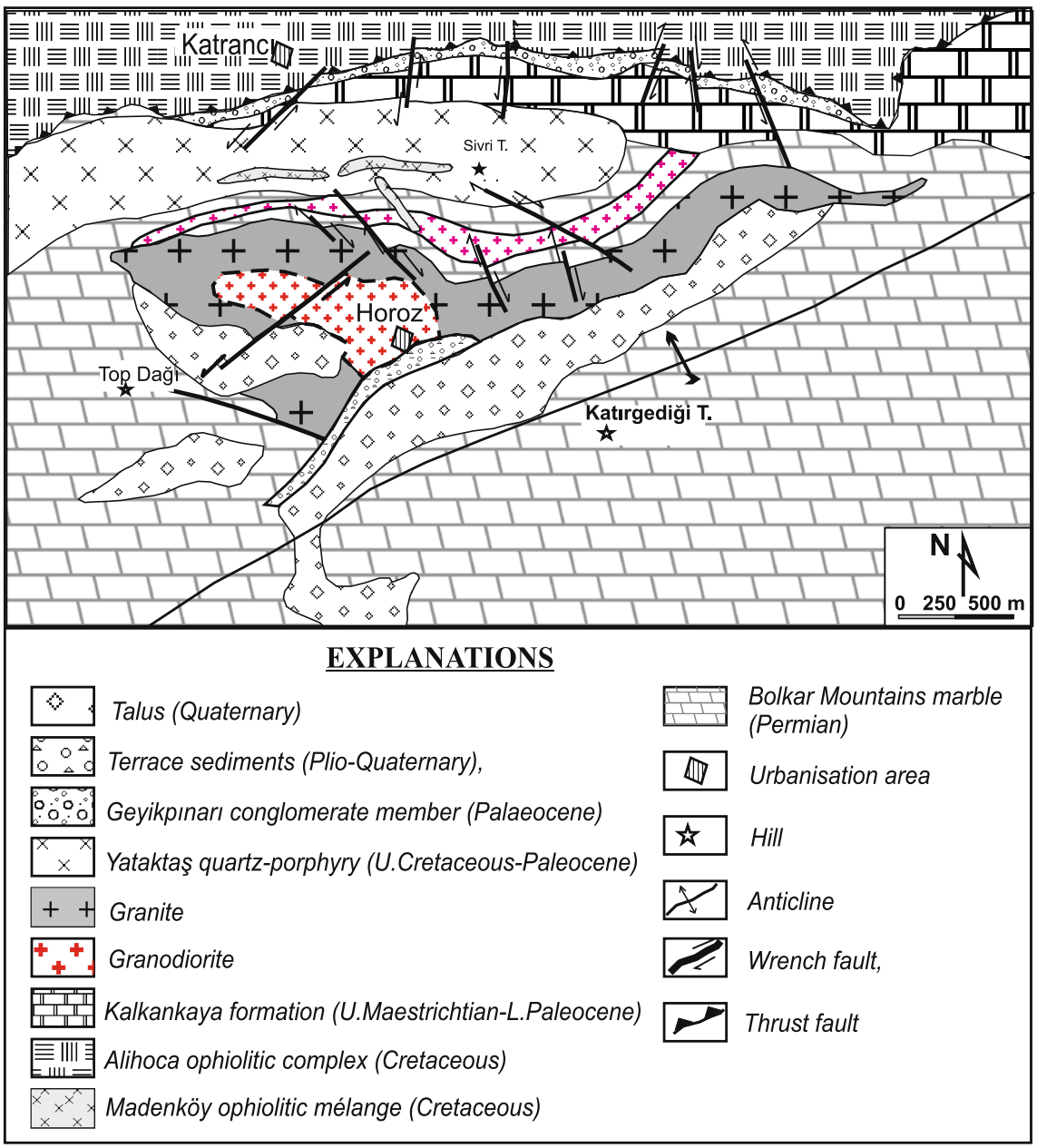

Fig. 2 Geological map of the study area (modified from Çevikbaş et al. 1995, and Kadioglu and Dilek 2009)

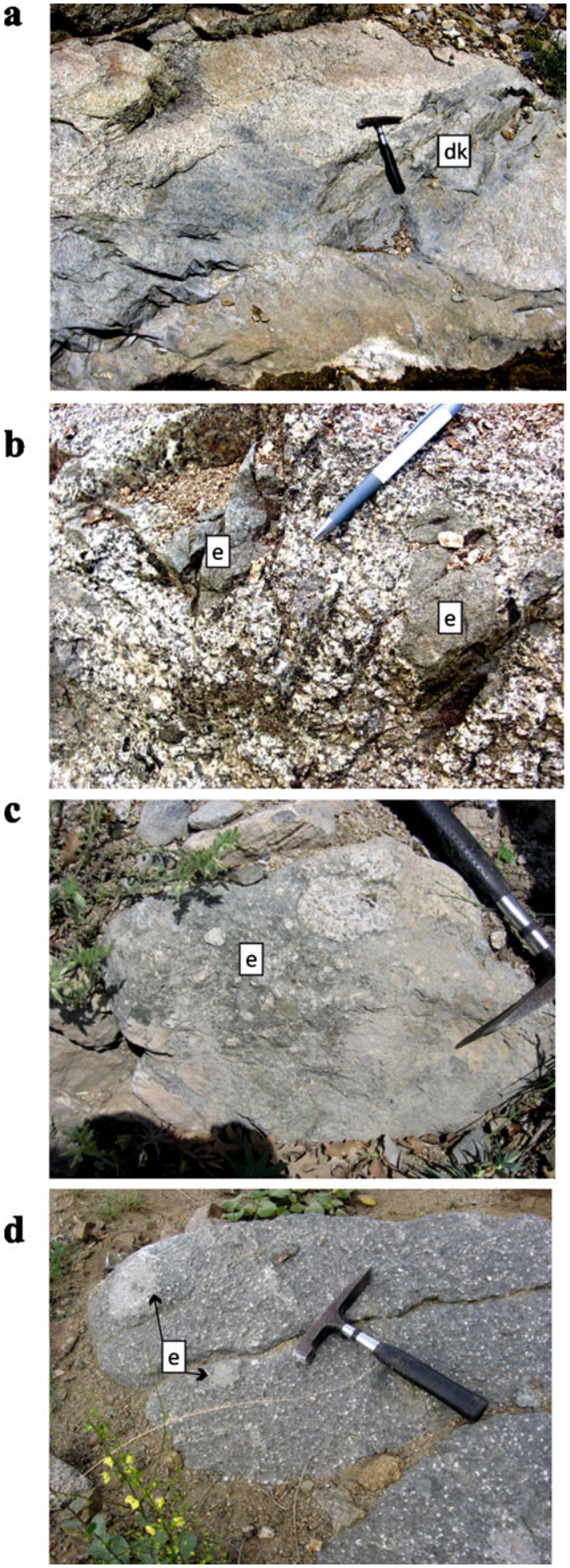

◀ **Fig. 3** Field photographs displaying **a** mafic dyke (dk); **b** MMEs displaying sharp contact with their host rock; **c** back veining in MME; **d** double enclave (**e**) in the dioritic dike

to be 56.1 Ma (earliest Eocene, Ypresian) using U–Pb zircon dating of its granitic end member (Y. Dilek, unpublished data; Kadioglu and Dilek 2009).

The granitoid is typically light-coloured and medium-fine grained with a slightly developed chilled margin at the contacts of the country rocks. This granitoid contains MMEs, which is suggestive of mingling in the felsic magma. Rare pelitic xenoliths with a diameter mostly less than 5 cm were also observed at the outermost margins of the pluton. Based on its mineralogical composition, the pluton can be classified into two distinct groups: granodiorite and granite (sensu stricto) with gradational contact. In comparison with the granodiorite, the felsic granite is relatively finer grained, more fractured and altered, and has less enclaves. The weathering can locally become intensive so as to produce sandy regoliths or grus.

The MMEs are rounded and tabular in shape, and their contacts with the host rocks are mostly sharp. In general, MMEs have dramatically different sizes (from several cm up to meters) and shapes (ellipse/round-cornered, Fig. 3b). Smaller MMEs tend to be finer grained and more isotropic than larger ones. The enclaves are less altered and are kept in better shape compared with the host granitoid. The MMEs are distributed randomly throughout the pluton. In no outcrops do the enclaves appear to be in any preferred alignment. The MMEs usually exhibit a fine-grained margin against the host rock, with sharp to crenulate contact. The enclaves sometimes show a core-tail structure in which the tails exhibit an S-shaped bend, implying that they were at least partly plastic when introduced into the felsic magma. Small blisters (1–10 cm in diameter) of the host rocks are incorporated into the MMEs (Fig. 3c). The feldspars are situated in the MMEs and near the host-enclave boundary. The MMEs in the dioritic dikes are texturally highly heterogeneous and may contain a "double enclave" structure in which they partially or fully enclose smaller, finer-grained, and more mafic enclaves (Fig. 3d).

In this study, we employ the terminology of Sparks and Marshall (1986), where 'magma mixing' produces homogeneous hybrid rocks and 'mingling' leads to inhomogeneous hybrid rocks.

Petrography and mineral chemistry

Methods

Sixty petrographic thin sections were studied under microscope to determine their composition and texture.

Polished sections (25 · 46 mm) of representative rock samples were made at the thin-section Laboratory of the Geological Engineering Department, Selcuk University (Konya). Polished slides were coated with carbon and then analysed at the Electron Microprobe Laboratory of McGill University, Montreal, Quebec, Canada. The mineral analyses were obtained using a JEOL JSM35 Electron Microprobe running Link QX2000 energy dispersive analytical software. The electron beam condition was 15 keV and 15 nA. The Fe^{3+} content in the amphiboles was determined according to Droop (1987).

General petrography

The granodiorite is composed of plagioclase (55–70 vol%), quartz (15–25%), biotite (5–15%), orthoclase (10–15%), amphibole (0–10%), minor chlorite, and apatite along with accessory apatite, tourmaline and zircon. The granite consists of zoned plagioclase (35–55 vol%), orthoclase (30–50%), quartz (15–30%), biotite (10–15%), amphibole (0–5%), and accessory apatite and zircon. In both granitoids, the hypidiomorphic granular texture is dominant, exhibiting various levels of sericitisation, chloritisation and kaolinitisation. The host rocks are sometimes highly fractured and altered, particularly in the granite, and the crystals are flattened by stretching or shearing, which produced the post-crystallisation features. Accordingly, the quartz crystals display strong undulose extinction and usually form numerous subgrains. The plagioclase may be slightly epidotised, particularly in its core. The quartz forms anhedral to the subhedral grains clustered between feldspar crystals, and it locally occurs as micrographic, granophyric and worm-like myrmekitic intergrowths. The biotite is usually subhedral, pleochroic from β-dark brown to α-pale yellow and contains inclusions of zircon. Amphibole is rare and is found only next to the contacts between the enclave and host rocks.

The MMEs have an almost identical mineral assemblage as their host. The main constituents are plagioclase (75–85%), amphibole (5–15%), biotite (5–10%), and orthoclase (0–5%), and the minor constituents are quartz, chlorite, titanite, clinozoisite, opaque iron ore and apatite (Fig. 4a–f). The MMEs are generally equigranular, fine-grained and sometimes porphyritic. Albite and albite-carlsbad twinnings are characteristic in the plagioclase, which may have sieve and boxy cellular textures (Fig. 4a–b). A poikilitic texture is characteristic in some samples that contain large euhedral-subhedral plagioclase and/or alkali feldspar (Fig. 4c) phenocrysts up to 2.0 mm in size, with the inclusion of subhedral biotite and amphibole. The K feldspar megacrysts are identical to those in the host, and they exhibit a perthitic texture and resorbtion. The quartz is interstitial and sometimes occurs as ocelli quartz, which is developed in the samples where the quartz crystals were engulfed by subhedral biotite, amphibole and/or feldspars (Fig. 4d). Quartz ovoids also exist in the samples. The amphibole frequently demonstrates conversion to brown biotite and chlorite (Fig. 4e) and is strongly altered into the chlorites along its cleavage, particularly in the granites. The titanite in the MMEs is predominantly anhedral to subhedral with an interstitial habit, but it sometimes forms typical wedge-shaped large crystal, up to 2.7 mm in maximum length, with plagioclase inclusion. Small subhedral titanite crystals are often associated with chlorite and opaque iron ore. The apatite has a typical acicular shape (Fig. 4f), suggesting quenching of the mafic melt globules trapped in silicic magma (Wyllie et al. 1962), but stubby prismatic shapes also exist.

The plagioclase in all samples is usually complexly zoned with a variety of compositional patterns; it shows a patchy zoned or resorbed slightly zoned core mantled by oscillatory zones, mostly planar and euhedral or gently curved (Fig. 5a–d). Electron microprobe traverses of the plagioclase show that many grains exhibit a distinct increase in An content (an An "spike", e.g., Wiebe 1968; Hibbard 1981), which interrupts and/or transects the normally zoned plagioclase. Two types of chemical zoning are determined in the zoning profiles: (a) in the first, the An content appears to increase from ~29 to ~41 and 38 to 49 between the core and rim respectively. (Fig. 5a–c), and there is a pronounced shift of ±<5 and ~15% of the An content in the outer part of the mantle at the granodiorite and enclave plagioclase, respectively (Fig. 5a, b and c); (b) in the second, the An content decreases regularly towards the rim (Fig. 5d). The oscillations within the rim are typically on the order of +25 and +22 mol% An in the MMEs and granodiorites, respectively. A sieve-textured zone that is 0.1–0.3 mm wide usually forms mantles on planar, locally fritted surfaces bounding oscillatory euhedral zones, sometimes with curvilinear boundaries.

Plagioclase

In the granitoids, the plagioclase occurs both as large euhedral crystals (up to 2.8*1.1 mm) and as small subhedral crystals (0.8*0.3 mm), usually with resorption features. The plagioclase composition of the granodiorites varies from An_{21} to An_{55} in the cores to An_{07}–An_{33} in the rims (Figs. 5 and 6, Table 1). The plagioclase composition of the granite is distinct from that of granodiorites, which varies from An_{17} to An_{38} in the core and from An_{18} to An_{24} in the rim (Table 1). The plagioclase crystal may exhibit albite twinning and/or normal zoning.

The MME plagioclase crystals ($An_{17–64}$, Fig. 5) are relatively smaller than those in their hosts, though some large crystals, up to 1.8 mm in size, form a poikilitic texture with numerous subhedral magnesiohornblende and biotite

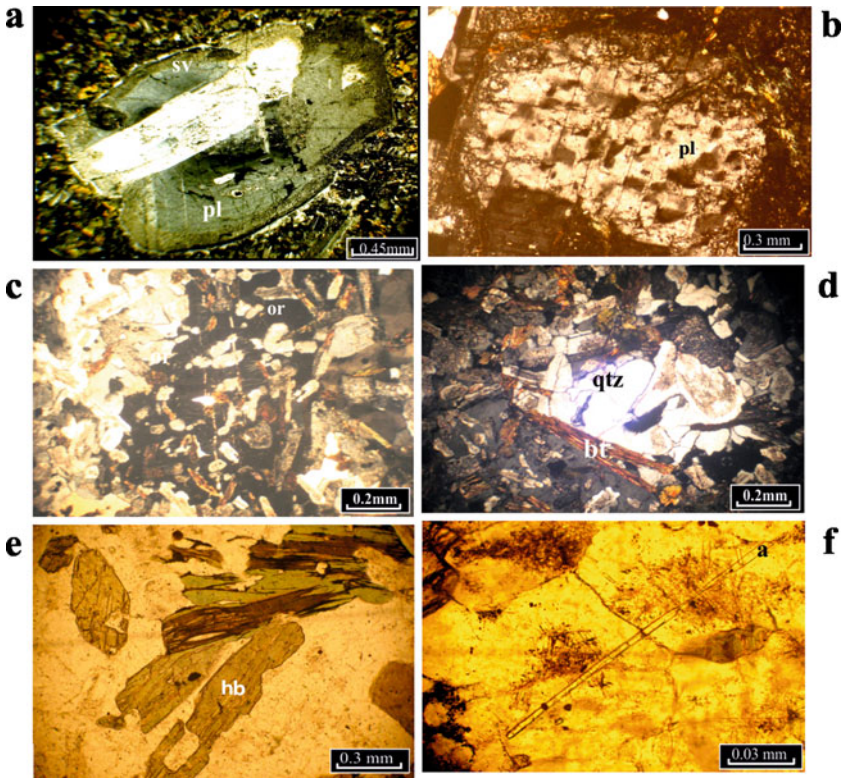

Fig. 4 Thin sections photographs of the MMEs (**a-f**) showing disequilibrium crystallization features and textures. **a** Plagioclase displaying sieve texture; **b** Boxy cellular plagioclase; **c** Orthoclase phenocryst with poikilitic texture and **d** Ocelli quartz; all photos under crossed polars. (**e**, **f**) Resorbed hornblende and acicular apatite (**f**) with quenched morphologies respectively (plane-polarized light). Quartz: *qtz*; orthoclase: *or*; plagioclase: *pl*; hornblende: *hb*; biotite: *bt*; *ap* apatite; *sv* sieve texture

inclusions. Their composition ranges from An_{18}–An_{64} in the cores to An_{17}–An_{29} in the rims (Figs. 5 and 6, Table 2). The compositional similarity between the plagioclase phenocrysts from the MMEs and their host rocks suggests that the MMEs were predominantly equilibrated with their hosts. The plagioclase inclusions in the K-feldspar megacrysts have a composition ranging from An_{55} to An_{27} in the cores and An_{22} to An_{19} in the rims.

Amphibole

The amphibole is usually subhedral and ranges in shape from blade to blocky in the granitoid and enclave samples. The enclave amphibole occurs in two grain sizes: (a) coarse-grained (2×0.7 mm) and (b) fine-grained (0.3×0.12 mm). In the IMA-approved nomenclature (Leake et al. 1997), both amphibole groups are classified as magnesio-hornblende and

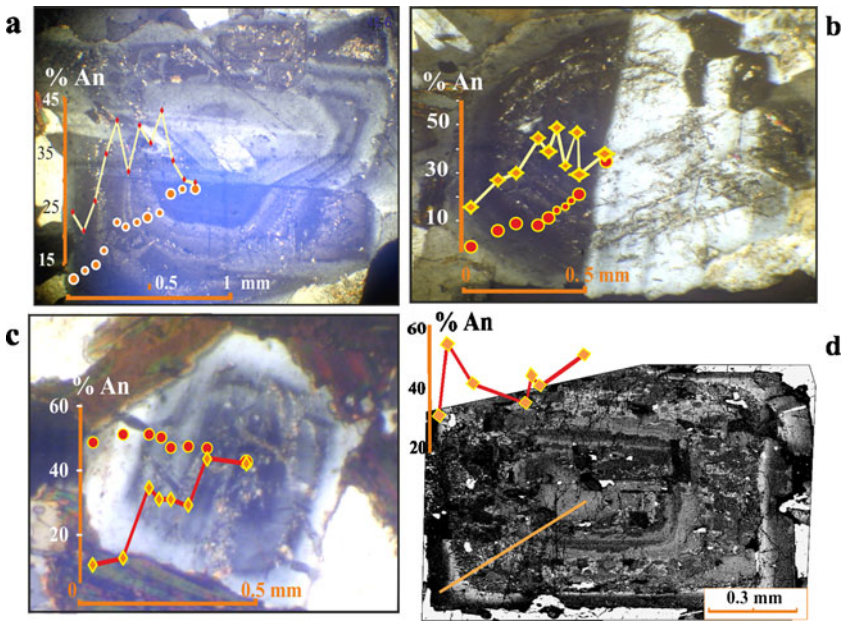

Fig. 5 The crossed polars image of the (**a**, **b**) Oscillatory zoning in plagioclase from granodiorites and enclave (**c**). **d** backscattered electron image of enclave plagioclase with oscillatory zoning

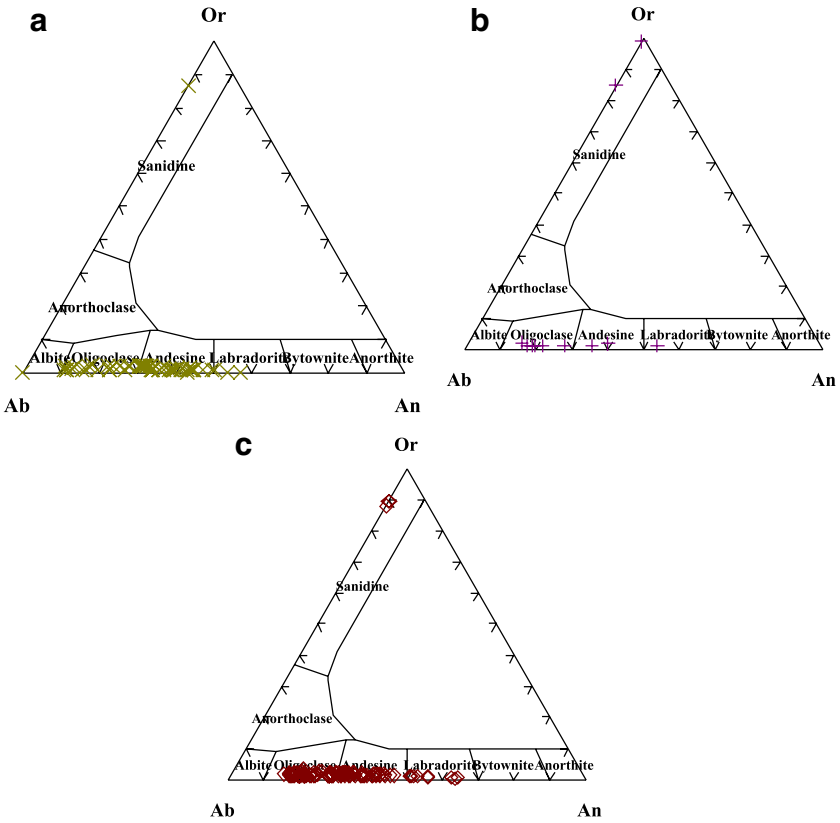

Fig. 6 Nomenclature of the feldspars from granodiorite (**a**), leucogranite (**b**) and MMEs (**c**)

edenite (Fig. 7a, b), which have high alkali (Na + K) contents and plot closer to the pargasitic substitution line (Fig. 7c) with an aluminium number (i.e., Al# = $^{[6]}Al/Al_T$) ≤ 0.21. The enclaves and their host also include unusual amphiboles, occasionally with Si>7.3, which is possibly not actually magmatic but rather the product of subsolidus reactions in the presence of an exsolved fluid (Chivas 1981; Hendry et al. 1985). The secondary amphiboles occur both as subhedral to anhedral homogeneous crystals or as patchy domains in the magnesiohornblende crystals (Fig. 7d), which show intensive resorption and some alteration to biotite. They are all magnesiohornblende in composition and rarely contain plagioclase inclusions. These Mg-rich amphiboles were possibly formed under conditions of high oxygen fugacity and were preferentially depleted in elements that partition into "late-magmatic" hydrothermal solutions.

In comparison with the amphibole of the granodiorites, the MME amphiboles have generally higher Al, Ti, Fe^{2+}, Ca, Na and K and lower Si and Fe^{3+}, Mg contents (Tables 3 and 4), though they nearly overlap in the classification diagram of Leake et al. (1997) (Fig. 7a), which may suggest that the amphibole has not been equilibrated. The amphibole phenocrysts from both groups demonstrate reverse zoning in terms of decreasing Mg/(Mg + Fe^{2+}), indicating the disequilibrium of crystallisation with magma (Fig. 7e). [Fe^{3+}/(Fe^{3+} + Mg)] = 0.32–0.52 for the Hbl in the MMEs, and [Fe^{3+}/(Fe^{3+} + Mg)] = 0.42–0.53 for the Hbl in the granodiorite. These ratios are much higher than 0.2 (Anderson and Smith 1995), suggesting crystallisation at high fO_2 for the granitoids and MMEs.

Biotite

Enclave biotite forms as phenocrysts (up to 1.02×0.7 mm) and as inclusions (0.2×0.13 mm) within the amphibole and plagioclase. This biotite varies in morphology from anhedral patches to subhedral blade-shaped crystals. The biotite is frequently bent and altered into green chlorite along its cleavage.

Representative analyses and calculated formulae of mica from the granodiorites and their MMEs are presented in Tables 5 and 6. All biotites show compositions with FeO= 18.24–20.26 wt.%, Al_2O_3=10.05–15.17 wt.%, and K_2O= 8.88–9.83 wt.% and can be classified as Fe-biotites and eastonite based on the classification diagram of Tischendorf et al. (1997) (Fig. 8a–d). The biotites are rich in TiO_2, with contents of 3.16–3.87 mass% in the enclaves and 3.29–3.92 mass% in the host rocks. The mole fractions of octahedrally coordinated Mg^{2+}, Fe^{2+}, and Fe^{3+} in the biotite of the MMEs and their host suggest that their nature is comparable to the primary biotite, which has been unaffected by hydrothermal alteration (Beane 1974). The FeO_t/MgO ratio

Table 1 Representative analyses of plagioclase from host rocks

Sample	Granite (45)											Granodiorite (29)							
	1-1								1-2			1-1		1–2		2-1			
	a	b	c	d	e	f	G	h	a	b	c	a	b	a	b	a	b	C	d
SiO_2	57.84	57.67	61.10	60.83	60.88	59.74	65.37	66.39	58.08	64.70	65.47	61.22	61.28	56.43	63.39	60.18	61.60	63.41	64.18
TiO_2	bdl	0.03	bdl	0.01	bdl	bdl	0.01	0.01	0.03	Bdl	0.05	0.02	bld	0.02	0.01	0.01	0.04	0.02	bld
Al_2O_3	26.59	26.69	24.50	24.81	24.62	25.04	21.63	21.02	26.52	22.23	21.56	24.16	24.43	27.22	22.78	24.94	24.15	22.65	22.15
FeO	0.24	0.26	0.13	0.12	0.15	0.14	0.16	0.11	0.18	0.13	0.13	0.15	0.27	0.17	0.20	0.18	0.13	0.14	0.09
BaO	0.02	0.02	0.02	0.01	0.08	0.03	0.02	bdl	0.03	bdl	bdl	0.07	0.02	0.04	0.05	0.06	0.06	bld	0.04
CaO	8.71	8.87	6.15	6.46	6.44	7.17	2.68	2.18	8.56	3.57	2.55	5.78	5.95	9.55	4.05	6.59	5.64	4.01	3.44
Na_2O	6.52	6.28	8.03	7.82	7.82	7.37	10.11	10.26	6.68	9.28	9.99	8.24	8.30	6.09	9.10	7.69	8.18	8.98	9.39
K_2O	0.27	0.25	0.36	0.30	0.31	0.31	0.28	0.35	0.21	0.44	0.22	0.24	0.20	0.22	0.20	0.37	0.22	0.49	0.31
Total	100.1	100.1	100.3	100.4	100.3	99.8	100.3	100.3	100.3	100.3	100.0	99.8	100.4	99.7	99.8	100.0	100.0	99.7	99.6
	Formula calculated for 32 O																		
Si	10.36	10.34	10.85	10.79	10.82	10.69	11.49	11.64	10.38	11.38	11.52	10.9	10.86	10.18	11.24	10.74	10.94	11.25	11.37
Al	5.61	5.63	5.12	5.18	5.15	5.28	4.48	4.34	5.58	4.61	4.47	5.07	5.10	5.78	4.76	5.239	5.05	4.734	4.62
Ti	bdl	0.00	bdl	0.00	bdl	bdl	0.00	0.00	0.00	bdl	0.01	0.00	bdl	0.00	0.00	0.00	0.00	0.00	bdl
Fe^{2+}	0.04	0.04	0.02	0.02	0.02	0.02	0.02	0.02	0.03	0.02	0.02	0.02	0.04	0.03	0.03	0.03	0.02	0.02	0.01
Ba	0.00	0.00	0.00	0.00	0.01	0.00	0.00	bdl	0.00	bdl	bdl	0.00	0.00	0.00	0.00	0.00	0.00	bdl	0.00
Ca	1.67	1.70	1.17	1.23	1.23	1.37	0.51	0.41	1.64	0.67	0.48	1.10	1.13	1.84	0.77	1.26	1.07	0.76	0.65
Na	2.26	2.18	2.76	2.69	2.69	2.55	3.45	3.49	2.31	3.17	3.41	2.85	2.85	2.13	3.13	2.66	2.82	3.09	3.23
K	0.06	0.06	0.08	0.07	0.07	0.07	0.06	0.08	0.05	0.10	0.05	0.05	0.04	0.05	0.04	0.08	0.0	0.11	0.07
Ab	56.60	55.30	68.80	67.50	67.50	63.90	85.90	87.80	57.80	80.40	86.50	71.1	70.9	52.9	79.4	66.5	71.5	77.9	81.7
An	41.80	43.20	29.10	30.80	30.70	34.30	12.60	10.30	41.00	17.10	12.20	27.5	28	45.8	19.5	31.5	27.3	19.3	16.5
Or	1.60	1.40	2.00	1.70	1.70	1.80	1.60	1.90	1.20	2.50	1.30	1.4	1.1	1.2	1.1	2.1	1.2	2.8	1.8

Table 2 Representative analyses of plagioclase from MMEs

Sample	13							17b									21a		
	1plg			2b	4plg			1plg		5-1	5-2	5-3	6-1	6-2	6-3		1-2		
	a	b	c		a	b	C	a	b						a	b	a	b	c
SiO_2	62.72	62.22	64.10	62.57	62.36	61.21	64.22	61.22	61.28	63.56	63.34	61.27	60.87	63.06	61.06	61.09	52.57	62.12	62.78
TiO_2	bld	0.03	bld	0.09	0.03	0.01	bld	0.02	bld	bld	bld	bld	bld	0.02	0.01	0.02	0.02	bld	bld
Al_2O_3	23.20	23.65	22.24	23.38	23.31	24.17	22.42	24.16	24.43	22.58	23.01	23.90	24.17	22.88	24.41	24.35	30.26	23.47	22.97
FeO	0.14	0.15	0.13	0.12	0.13	0.13	0.22	0.15	0.27	0.14	0.23	0.12	0.23	0.22	0.07	0.11	0.18	0.14	0.21
BaO	0.03	0.02	0.02	0.02	bld	0.04	0.01	0.07	0.02	bld	bld	0.07	0.03	bld	0.03	0.03	0.02	0.02	bld
CaO	4.64	5.05	3.65	5.01	4.88	5.96	3.81	5.78	5.95	4.04	4.21	5.74	6.06	4.11	5.97	5.83	12.95	5.11	4.41
Na_2O	8.87	8.42	9.32	8.76	8.66	8.20	9.55	8.24	8.30	9.05	9.00	8.05	8.21	9.12	8.16	8.32	4.14	8.59	8.97
K_2O	0.27	0.46	0.38	0.23	0.27	0.29	0.18	0.24	0.20	0.42	0.26	0.39	0.19	0.21	0.21	0.15	0.07	0.31	0.23
Total	99.9	100	99.8	100.1	99.6	100.0	100.4	99.8	100.4	99.8	100.0	99.5	99.5	99.5	99.9	99.9	100.1	99.8	99.6
	Formula calculated for 32 O																		
Si	11.13	11.04	11.34	11.08	11.09	10.89	11.31	10.9	10.86	11.27	11.2	10.95	10.86	11.2	10.87	10.87	9.517	11.05	11.17
Al	4.85	4.94	4.63	4.87	4.88	5.06	4.65	5.07	5.10	4.71	4.79	5.03	5.08	4.79	5.12	5.10	6.45	4.92	4.81
Ti	bdl	0.00	bdl	0.013	0.00	0.00	bdl	0.00	bdl	bdl	bdl	bdl	bdl	0.00	0.00	0.00	0.00	bdl	bdl
Fe^{2+}	0.02	0.02	0.02	0.02	0.02	0.02	0.03	0.02	0.04	0.02	0.03	0.02	0.03	0.03	0.01	0.02	0.03	0.02	0.03
Ba	0.00	0.00	0.00	0.00	bdl	0.00	0.00	0.00	0.00	bdl	bdl	0.00	0.00	bdl	0.00	0.00	0.00	0.00	bdl
Ca	0.88	0.96	0.69	0.95	0.93	1.14	0.72	1.10	1.13	0.77	0.80	1.10	1.16	0.78	1.14	1.11	2.51	0.97	0.84
Na	3.05	2.90	3.20	3.01	2.99	2.83	3.26	2.85	2.85	3.11	3.09	2.79	2.84	3.14	2.81	2.87	1.45	2.96	3.09
K	0.06	0.10	0.09	0.05	0.06	0.06	0.04	0.05	0.04	0.09	0.06	0.09	0.04	0.05	0.05	0.03	0.01	0.07	0.05
Ab	76.4	73.1	80.4	75	75.1	70.2	81.1	71.1	70.9	78.3	78.3	70.2	70.3	79.1	70.3	71.5	36.5	73.9	77.6
An	22.1	24.2	17.4	23.7	23.4	28.2	17.9	27.5	28	19.3	20.2	27.6	28.7	19.7	28.5	27.7	63.1	24.3	21.1
Or	1.5	2.7	2.2	1.3	1.5	1.6	1.0	1.4	1.1	2.4	1.5	2.2	1.0	1.2	1.2	0.9	0.4	1.8	1.3

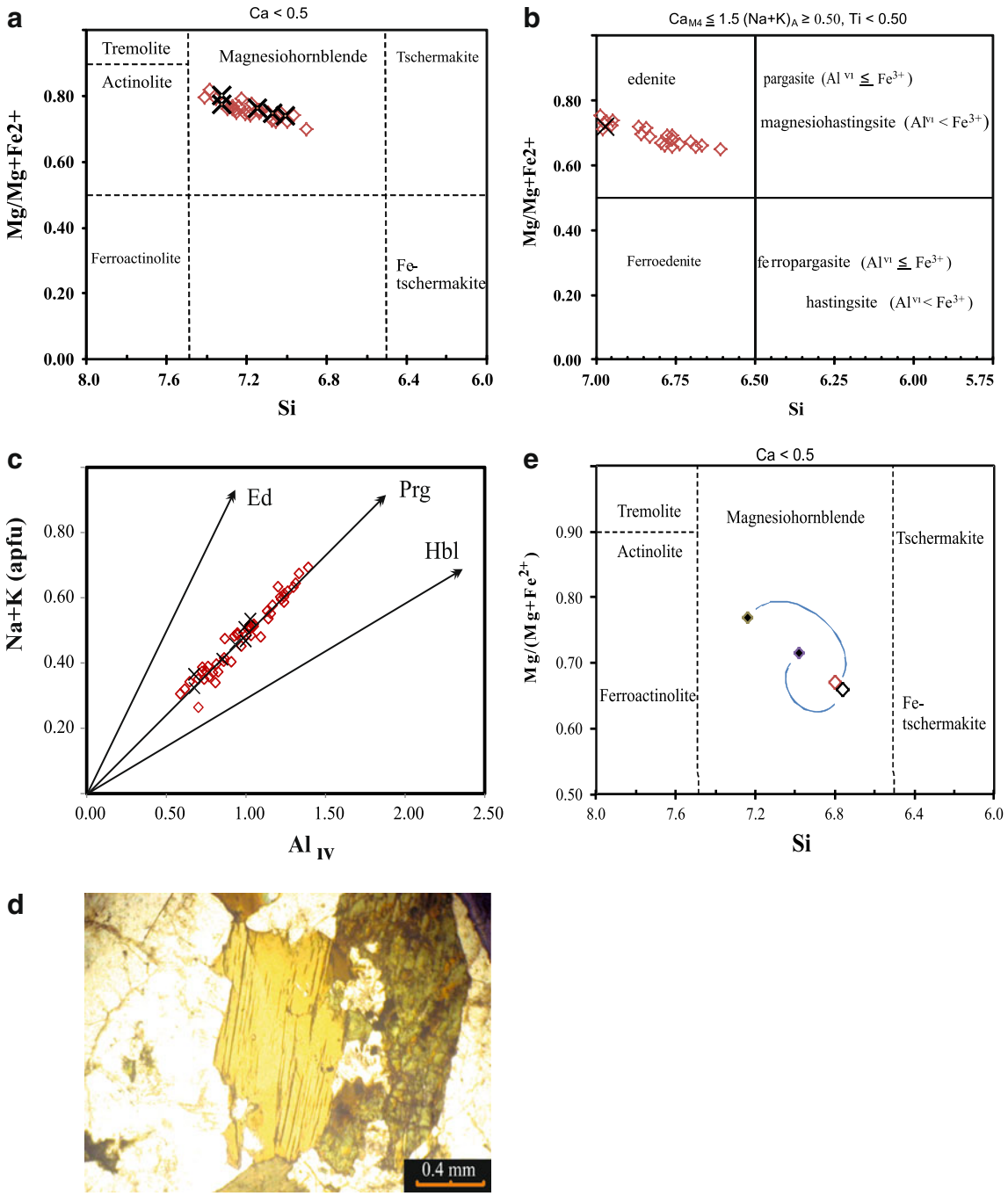

Fig. 7 **a**, **b** Nomenclatures of the amphiboles (Leake et al. 1997). **c** Na + K vs. Al^{iv}. Edenitic (Ed), pargasitic (Prg), and tschermakitic (Ts) substitutions are indicated along with an idealised hornblende (Hbl) substitution (Hietanen 1974). **d** Patchy domains in the hornblende refer to secondary hornblende. **e** Inverse chemical zoning from enclaves amphiboles. *Filled and open diamonds* represent rim and core of the enclave hornblendes, respectively. X: granodiorite ◊: enclave

of biotites in the granodiorite and MMEs ranges between 1.30 and 1.55, with an average of 1.41, and between 1.27 and 1.46, with an average of 1.37, respectively. These values are close to those of the Mg–biotites (FeOt/MgO= 1.76) typically associated with calcic pyroxene and/or calcic amphibole commonly found in calc–alkaline (mostly orogenic and subduction-related) I-type granitoid suites (Abdel-Rahman 1994). The Fe^{2+}/Fe^{2+} + Mg ratio and the iron-enrichment index of biotite in the host granodiorite are identical to the biotite in the MMEs, suggesting that the biotites could be entirely equilibrated with the MMEs. The SiO_2 content of the samples also supports this suggestion, as it ranges from 36.26 to 37.08 mass% and 35.12 to 36.97 mass% in the enclaves and granodiorites, respectively.

Table 3 Representative analyses of the hornblende from granodiorite (Sample 40b)

Sample	2-hb-a	2-hb-b	3hb-a	3hb-c	3hb-b	4-1hb	4-2hb
SiO_2	47.76	49.93	47.11	49.99	48.33	47.35	47.75
TiO_2	0.94	0.66	1.00	0.62	0.87	0.94	0.95
Al_2O_3	6.17	4.66	7.19	4.67	5.69	6.94	6.87
Fe_2O_3	7.05	7.23	7.10	8.17	7.39	7.39	7.09
FeO	8.40	7.59	8.99	6.54	7.83	8.41	8.72
MnO	0.90	0.95	0.90	1.00	0.87	0.86	0.87
MgO	13.78	14.53	13.03	14.82	14.07	13.38	13.53
CaO	11.58	11.37	11.32	11.37	11.47	11.48	11.50
Na_2O	1.24	1.04	1.51	0.88	1.10	1.27	1.41
K_2O	0.54	0.38	0.53	0.40	0.51	0.54	0.57
Total	98.36	98.32	98.67	98.43	98.13	98.57	99.26
	Formula calculated for 23 O						
Si	7.07	7.33	6.97	7.32	7.15	7.00	7.01
Al ^{iv}	0.93	0.68	1.03	0.68	0.85	1.00	0.99
Al ^{vi}	0.14	0.13	0.23	0.13	0.14	0.2	0.20
Ti	0.10	0.07	0.11	0.07	0.10	0.11	0.11
Fe $^{3+}$	0.79	0.80	0.79	0.90	0.82	0.82	.78
Mg	3.04	3.18	2.88	3.24	3.10	.95	2.96
Fe $^{2+}$	0.93	0.82	1.00	0.67	0.84	0.91	0.95
Fe^{2+}	0.11	0.11	0.11	0.14	0.13	0.13	0.12
Mn	0.11	0.12	0.11	0.12	0.11	0.11	0.11
Ca	1.77	1.77	1.77	1.74	1.76	1.76	1.78
Na	0.36	0.29	0.43	0.25	0.32	0.37	0.40
K	0.10	0.07	0.10	0.07	0.10	0.10	0.11
$Mg/(Mg + Fe^{2+})$	0.74	0.77	0.72	0.80	0.76	0.74	0.73

The MICA+ (Yavuz 2003) computer programs were utilised for the mineralogical calculations of the mica analyses. The micas analysed from the enclave and their hosts are all trioctahedral micas ($2.74 \leq M$ site <2.95 atoms per formula unit) and, for the most part, eastonite. Figure 8c and d show the octahedrally coordinated cations in the terms of Foster (1960). Biotites are found on the line along which the Mg:Fe ratio is 1:1.

Structural formulae calculated based on 22 positive charges show that the Si and Al cation p.f.u. usually fills the tetrahedral sites. In contrast, the sum of octahedral sites show somewhat more variability, particularly in enclaves, between 2.89 and 3.09 cations p.f.u. The occupation of 12-fold coordination sites ranges between 0.867 to 1.397 and 0.917 to 0.973 in the enclaves and their host, respectively. All these values suggest that all micas are near the ideal stoichiometric values.

The Fe^{3+} contents and $Fe_{tot}/(Fe_{tot} + Mg)$ ratios give at least relative information about the oxygen fugacity during crystallisation (Wones and Eugster 1965; Dodge et al. 1969; Albuquerque 1973; Barriere and Cotten 1979; Neiva 1981). Both groups of biotites plot above the Ni-NiO (NNO) oxygen fugacity buffer (Fig. 9a, b) in the Fe^{2+}-Fe^{3+}-Mg diagram of Wones and Eugster (1965), indicating moderately oxidising conditions.

Abdel-Rahman (1994) introduces discrimination diagrams on the basis of the major-element composition of biotite in igneous rocks crystallised from three distinct magma types. The biotites in granodiorites and enclaves in terms of MgO FeO_t Al_2O_3 components show their crystallisation in a subduction-related calc-alkaline magma (Figs. 9a, b and 10).

Discussion

The mineralogical compositions of the MMEs are fairly comparable to those of the host granites. The ubiquitous finer grain size of the enclaves and the lack of cumulate texture are inconsistent with their being cumulates (Barbarin and Didier 1992). The enclaves do not include sillimanite, andalusite, cordierite, garnet or residual minerals produced from mica dehydration melting. Consequently, they do not represent restite. Correspondingly, a combination of characteristics such as an elliptical to rounded shape, contact morphologies (such as phenocrysts of host granites partly enclosed in MMEs and host granite magma), and igneous microtextures with acicular apatite strongly suggest that the MMEs may represent remnants of a mafic component added to intermediate or felsic magma chambers (Eichelberger 1980; Vernon

Table 4 Representative analyses of amphiboles from MMEs

Sample	21a-1-1		21a-2		24b				17b-1					
	a	b	a	b	1.1	4-1-a	4-1-b	4-1-c	1-a	1-b	1-c	2	3–1	5–2
SiO_2	43.96	45.02	45.17	47.00	48.04	45.53	49.24	49.29	48.92	47.89	49.30	48.32	46.34	45.62
TiO_2	1.42	1.24	1.28	1.06	1.21	1.25	0.80	0.66	0.59	0.90	0.58	0.80	0.99	1.11
Al_2O_3	9.34	9.20	8.61	6.90	5.51	8.16	5.08	5.15	5.74	6.30	5.67	5.86	7.51	7.96
Fe_2O_3	6.73	6.55	5.62	6.64	7.09	5.60	6.64	6.32	7.40	6.25	6.57	7.04	6.42	6.65
FeO	10.89	10.87	10.99	9.37	8.03	10.75	7.83	8.47	7.40	8.33	8.59	8.07	9.73	9.89
MnO	0.91	0.84	0.81	0.82	1.09	0.89	0.92	1.01	0.87	0.84	0.76	0.82	0.87	0.85
MgO	11.38	11.69	11.87	13.11	13.88	12.23	14.59	14.23	14.51	13.94	14.21	14.08	12.74	12.35
CaO	11.42	11.55	11.56	11.48	11.23	11.54	11.62	11.68	11.74	11.71	11.81	11.59	11.76	11.43
Na_2O	1.66	1.59	1.41	1.33	1.25	1.58	1.04	1.00	1.00	1.02	0.99	1.09	1.18	1.43
K_2O	1.10	0.99	0.93	0.70	0.61	0.93	0.49	0.47	0.47	0.59	0.48	0.55	0.74	0.84
Total	98.81	99.54	98.25	98.41	97.95	98.47	98.24	98.25	98.65	97.77	98.95	98.20	98.26	98.14
	Formula calculated for 23 O													
Si	6.61	6.69	6.76	6.98	7.13	6.80	7.24	7.25	7.17	7.09	7.21	7.14	6.91	6.83
Al ^{iv}	1.39	1.31	1.24	1.02	0.87	1.20	0.76	0.75	0.83	0.91	0.79	0.86	1.09	1.17
Al ^{vi}	0.26	0.30	0.28	0.19	0.10	0.23	0.12	0.14	0.17	0.19	0.18	0.16	0.23	0.24
Ti	0.16	0.14	0.14	0.12	0.14	0.14	0.09	0.07	0.07	0.10	0.06	0.09	0.11	0.13
Fe $^{3+}$	0.76	0.73	0.63	0.74	0.79	0.63	0.73	0.70	0.82	0.70	0.72	0.78	0.72	0.75
Mg	2.55	2.59	2.65	2.90	3.07	2.72	3.20	3.12	3.17	3.08	3.10	3.10	2.83	2.76
Fe $^{2+}$	1.27	1.25	1.30	1.05	0.91	1.28	0.87	0.97	0.78	0.94	0.94	0.87	1.12	1.13
Fe $^{2+}$	0.10	0.10	0.08	0.11	0.09	0.07	0.10	0.08	0.13	0.09	0.11	0.12	0.10	0.11
Mn	0.12	0.11	0.10	0.10	0.14	0.11	0.12	0.13	0.11	0.11	0.09	0.10	0.11	0.11
Ca	1.78	1.79	1.82	1.79	1.77	1.82	1.79	1.80	1.77	1.80	1.79	1.78	1.79	1.79
Na	0.48	0.46	0.41	0.38	0.36	0.46	0.30	0.29	0.29	0.29	0.28	0.31	0.34	0.42
K	0.21	0.19	0.18	0.13	0.12	0.18	0.09	0.09	0.09	0.11	0.09	0.10	0.14	0.16
P(kbar)	4.11	3.92	3.51	2.13	1.06	3.15	0.69	0.74	1.19	1.66	1.11	1.31	2.63	3.00
T^0C(ed-tr)					783		764	739		730		788	808	869
T^0C(ed-ri)					940		925	884		818		918	852	917

Pressure (P) calculated with the Al-in-hornblende barometry (Anderson and Smith 1995). Temperatures T (edenite-tremolite) and Temperatures T (edenite-richterite) are calculated with Hornblende-plagioclase thermometer of Holland and Blundy (1994)

1984; Didier and Barbarin 1991; Bonin 2004; Barbarin 2005; Yang et al. 2006, 2007; Qin et al. 2009).

The magma mixing has been suggested from a number of lines of evidence:

(1) The coexistence of contrasting magmas may be suggested by the chilling of the basic mass and disrupted late syn-plutonic dykes or an abundance of mafic microgranular enclaves (Didier 1973; Vernon 1984; Didier and Barbarin 1991; Wiebe 1996). In a slowly cooled and intrusive environment, the quenched texture could be in part obscured by recrystallisation effects (e.g., Wall et al. 1987). Alternatively, the breakdown of larger enclaves with chilled margins could create many smaller ones that mainly lack the chilled margins. Enclave magma quenching against the cooler felsic host is indicated by the shape of the enclaves, which are rounded to ovoid, subangular to angular and have lobes that are convex towards the host granitoids. Vernon et al. (1988) have stressed that rounded- to ellipsoidal-shaped enclaves are a strong sign of magma mingling and flow.

(2) The preliminary quenching and multistage crystallisation of the assumed hybrids can be shown by the acicular apatite and blade-like biotite, together with quartz and K-feldspar megacrysts with many inclusions of biotite and amphibole (Vernon 1990, 1991; Hibbard 1991, 1995). Wyllie et al. (1962) experimentally showed that long prismatic-acicular crystals could result from strong undercooling during growth, and this is mostly taken as indirect evidence of magma mixing, showing the quenching of the basic melt by cooler acidic magma (Didier 1987; Hibbard 1991, 1995). The poikilitic texture in the enclaves is also possibly the result of the late stage crystallisation of felsic melt following the

Table 5 Representative analyses of biotite from the granodiorites

Sample	40b1		40b2-1		40b2-2	40b2-2		47-2-1	47-2-2	47-4	
	a	b	a	b		a	b			a	b
SiO_2	36.97	36.88	36.25	36.47	36.82	36.61	36.96	35.12	36.02	36.25	36.41
TiO_2	3.76	3.29	3.81	3.92	3.87	3.80	3.85	3.78	3.30	3.84	3.71
Al_2O_3	14.27	14.51	14.13	10.05	13.94	14.71	14.57	15.17	14.81	13.95	14.13
FeO	18.32	18.24	18.66	18.52	18.60	19.60	19.39	20.26	19.51	19.90	19.78
MnO	0.57	0.56	0.52	0.54	0.57	0.45	0.48	0.51	0.46	0.58	0.60
MgO	12.27	12.60	12.52	12.38	12.85	11.84	12.07	11.75	11.96	12.17	12.07
CaO	0.08	0.12	0.01	0.06	0.02	bdl	0.01	bdl	0.02	0.04	0.01
Na_2O	0.08	0.09	0.09	0.10	0.12	0.09	0.08	0.07	0.06	0.15	0.07
K_2O	9.28	9.24	9.52	9.30	9.54	9.65	9.83	9.76	9.39	9.63	9.55
Total	95.60	95.53	95.51	91.34	96.33	96.75	97.24	96.42	95.53	96.51	96.33
	Formula calculated for 11 O										
Si	2.80	2.80	2.77	2.93	2.78	2.77	2.78	2.68	2.76	2.76	2.77
Al ^{iv}	1.20	1.20	1.23	0.95	1.22	1.24	1.22	1.32	1.25	1.24	1.23
Al ^{vi}	0.08	0.10	0.04	0.00	0.03	0.08	0.07	0.05	0.09	0.01	0.04
Ti	0.21	0.19	0.22	0.24	0.22	0.22	0.22	0.22	0.19	0.22	0.21
Fe $^{2+}$	0.87	0.89	0.81	0.91	0.80	0.92	0.91	0.84	0.91	0.87	0.88
Fe $^{2+}$	0.29	0.27	0.38	0.21	0.38	0.32	0.30	0.46	0.34	0.40	0.38
Mn	0.04	0.04	0.03	0.04	0.04	0.03	0.03	0.03	0.03	0.04	0.04
Mg	1.39	1.43	1.43	1.48	1.45	1.33	1.35	1.34	1.36	1.38	1.37
Total (M)	3.04	3.06	3.04	3.02	3.06	3.04	3.04	3.02	3.04	3.05	3.05
Ca	bld	0.01	bld	Bld	bld	bld	bld	bld	bld	bld	bld
Na	0.01	0.01	0.01	0.02	0.02	0.01	0.01	0.01	bld	0.02	0.01
K	0.90	0.89	0.93	0.95	0.92	0.93	0.94	0.95	0.92	0.94	0.93
Total(I)	0.92	0.92	0.94	0.97	0.94	0.94	0.96	0.96	0.93	0.96	0.94
Xph	0.15	0.14	0.17	0.15	0.17	0.16	0.15	0.18	0.15	0.18	0.17
Xmn	0.01	0.01	0.01	0.01	0.01	bld	0.01	0.01	0.01	0.01	0.01
Xal	0.03	0.03	0.01	0.00	bld	0.03	0.02	0.02	0.03	bld	0.01
Xti	0.07	0.06	0.07	0.08	0.07	0.07	0.07	0.07	0.06	0.07	0.07
I.E.	0.46	0.46	0.46	0.46	0.46	0.49	0.48	0.50	0.48	0.49	0.49
Mg#	0.54	0.55	0.55	0.54	0.55	0.52	0.53	0.51	0.52	0.52	0.52
$Fe^{2+}/Fe^{2+}Fe^{3+}$	0.75	0.77	0.68	0.74	0.68	0.74	0.75	0.65	0.73	0.68	0.70

T, M, I, and A refer to tetrahedral, octahedral, interlayer and anions positions according to the IMA nomenclature for micas (Rieder 2001). Xph, Xan, Xpdo, Xmn, Xal, Xti = Mole fractions of phlogopite, annite, protondeficient oxyannite, manganobiotite, aluminobiotite and titanobiotite determined on the basis of all octahedral ions (calculated according to Jacobs and Parry 1979). Iron-enrichment index (I.E.) = (Fe + Mn)/(Fe + Mn + Mg)

Mica end-member calculations (wt.%) of talc, Ti-phlogopite, ferri-eastonite, muscovite, eastonite, and phlogopite calculated according to Dymek (1983)

crystallisation of numerous quench-generated amphibole and biotite in relation to magma mixing (Hibbard 1991).

(3) An exchange of crystals (xenocrysts) is displayed by plagioclases and amphibole with resorption surfaces, quartz ocelli rimmed by biotite and amphibole, quartz ovids, and a sieve texture. The quartz ocelli are developed by the partial dissolution of quartz xenocrysts in the mafic magma that extracts latent heat from the adjacent liquid. The undercooled surface of the quartz grain was transformed into a preferential nucleation substrate for minerals of the mafic magma (Vernon 1990). The sieve texture may be developed in at least two ways. If a plagioclase crystal is put into a magma in which it is not in equilibrium (by magma mixing, Wiebe 1968; Pringle et al. 1974; Tsuchiyama 1985; Nelson and Montana 1992), then it will become corroded, and melt will move into the crystal structure. New plagioclase of a distinct composition will crystallise from the magma and possibly form a rim around the corroded core. The sieve texture may also be formed by decompression when magma rises towards the surface (Stomer 1972). The exchange of crystals is also displayed by overgrowths

Table 6 Representative analyses of the biotite from the MMEs. For explanations see Table 5

Sample	3-1		3-2	4-1						5-1	
	A	b		a	b	c	d	e	f	a	b
SiO_2	36.75	36.82	36.73	36.36	36.59	36.54	36.62	36.31	36.44	36.51	36.57
TiO_2	3.50	3.47	3.33	3.76	3.67	3.72	3.51	3.63	3.16	3.69	3.62
Al_2O_3	14.54	14.44	14.15	13.95	14.16	14.65	14.45	14.77	15.01	14.29	14.42
FeO	18.86	18.80	18. 55	19.17	19.08	18.84	18.66	19.22	19.43	19.73	19.44
MnO	0.26	0.28	0.37	0.59	0.47	0.50	0.50	0.58	0.53	0.39	0.34
MgO	12.67	12.33	12.67	12.50	12.61	12.15	12.51	12.53	12.34	12.14	12.40
CaO	Bdl	0.05	bdl	0.02	bdl	0.01	0.02	0.05	bdl	0.01	0.01
Na_2O	0.06	9.68	0.07	0.09	0.08	0.07	0.06	0.06	0.05	0.07	0.08
K_2O	9.58	9.68	9.76	9.48	9.69	9.70	9.49	9.44	8.88	9.57	9.66
Total	96.22	95.87	95.60	95.92	96.35	96.18	95.82	96.59	95.84	96.40	96.54
	Formula calculated for 11 O										
Si	2.78	2.73	2.80	2.77	2.77	2.77	2.78	2.74	2.77	2.77	2.77
Al ^{iv}	1.22	1.26	1.20	1.23	1.23	1.23	1.22	1.26	1.24	1.23	1.23
Al ^{vi}	0.07	0.00	0.07	0.02	0.04	0.08	0.07	0.06	0.11	0.05	0.05
Ti	0.20	0.19	0.19	0.22	0.21	0.21	0.20	0.21	0.18	0.21	0.21
Fe $^{2+}$	0.87	0.97	0.91	0.82	0.85	0.89	0.86	0.81	0.84	0.89	0.88
Fe $^{2+}$	0.32	0.20	0.27	0.40	0.36	0.30	0.32	0.41	0.39	0.36	0.35
Mn	0.02	0.02	0.02	0.04	0.03	0.03	0.03	0.04	0.03	0.03	0.02
Mg	1.43	1.37	1.44	1.42	1.43	1.37	1.42	1.41	1.40	1.37	1.40
Total (M)	3.06	2.89	3.05	3.05	3.06	3.03	3.05	3.06	3.09	3.05	3.05
Ca	0.00	0.00	bdl	0.00	bdl	0.00	0.00	0.00	bdl	0.00	0.00
Na	0.01	1.39	0.01	0.01	0.01	0.01	0.01	0.01	0.01	0.01	0.01
K	0.92	0.93	0.95	0.92	0.94	0.94	0.92	0.91	0.86	0.93	0.93
Total(I)	0.93	1.40	0.96	0.94	0.95	0.95	0.93	0.92	0.87	0.94	0.95
Xph	0.47	0.47	0.47	0.47	0.47	0.45	0.46	0.46	0.45	0.45	0.46
Xmn	0.01	0.01	0.01	0.01	0.01	0.01	0.01	0.01	0.01	0.01	0.01
Xal	0.02	0.00	0.02	0.01	0.01	0.03	0.02	0.02	0.04	0.02	0.02
Xti	0.07	0.07	0.06	0.07	0.07	0.07	0.07	0.07	0.06	0.07	0.07
I.E.	0.46	0.47	0.46	0.47	0.47	0.47	0.46	0.47	0.48	0.48	0.47
Mg#	0.55	0.54	0.55	0.54	0.54	0.54	0.54	0.54	0.53	0.52	0.53
$Fe^{2+}/Fe^{2+}Fe^{3+}$	0.73	0.83	0.77	0.67	0.70	0.75	0.73	0.67	0.68	0.71	0.72

and sharp zoning discontinuities (compositional spikes) in the plagioclase (e.g., King 1964; Wiebe 1968; Hibbard 1981; Barbarin 1990; Baxter and Feely 2002; Kocak 2006). Many plagioclase grains in the MMEs show evidence of resorption or dissolution and the subsequent re-growth of zones of differing An composition. These processes caused the formation of boxy cellular plagioclase (Figs. 4b), which may develop when plagioclase, originating from the mafic material, comes in contact with the cooler, felsic magma (Hibbard 1995). The plagioclase is then converted into more sodic compositions as equilibration occurs.

The homogenisation of the interacting melt phases results in the conversion of any pre-existing crystals to minerals stable in hybrid melt (enclave environment) or their rimming by stable minerals (e.g., Reid et al. 1983; Vernon 1983, 1984). Thus, the compositionally similar biotite and the similar sodic rims on the zoned plagioclase in the host rocks and their enclaves were developed. The high-level emplacement of the Horoz magma led to its saturation with H_2O and the exsolution of fluids at an early stage of crystallisation. According to Blundy and Sparks (1992) and Waight et al. (2001), the diffusion of alkalis and water is much faster than that of other components, which promotes the crystallisation of biotite at the expense of amphibole. Finally, the dissolution of xenocrysts takes place in a new hybrid (enclave) magma environment, giving way to a reduction in grain size and the formation of ocellar mineral grains.

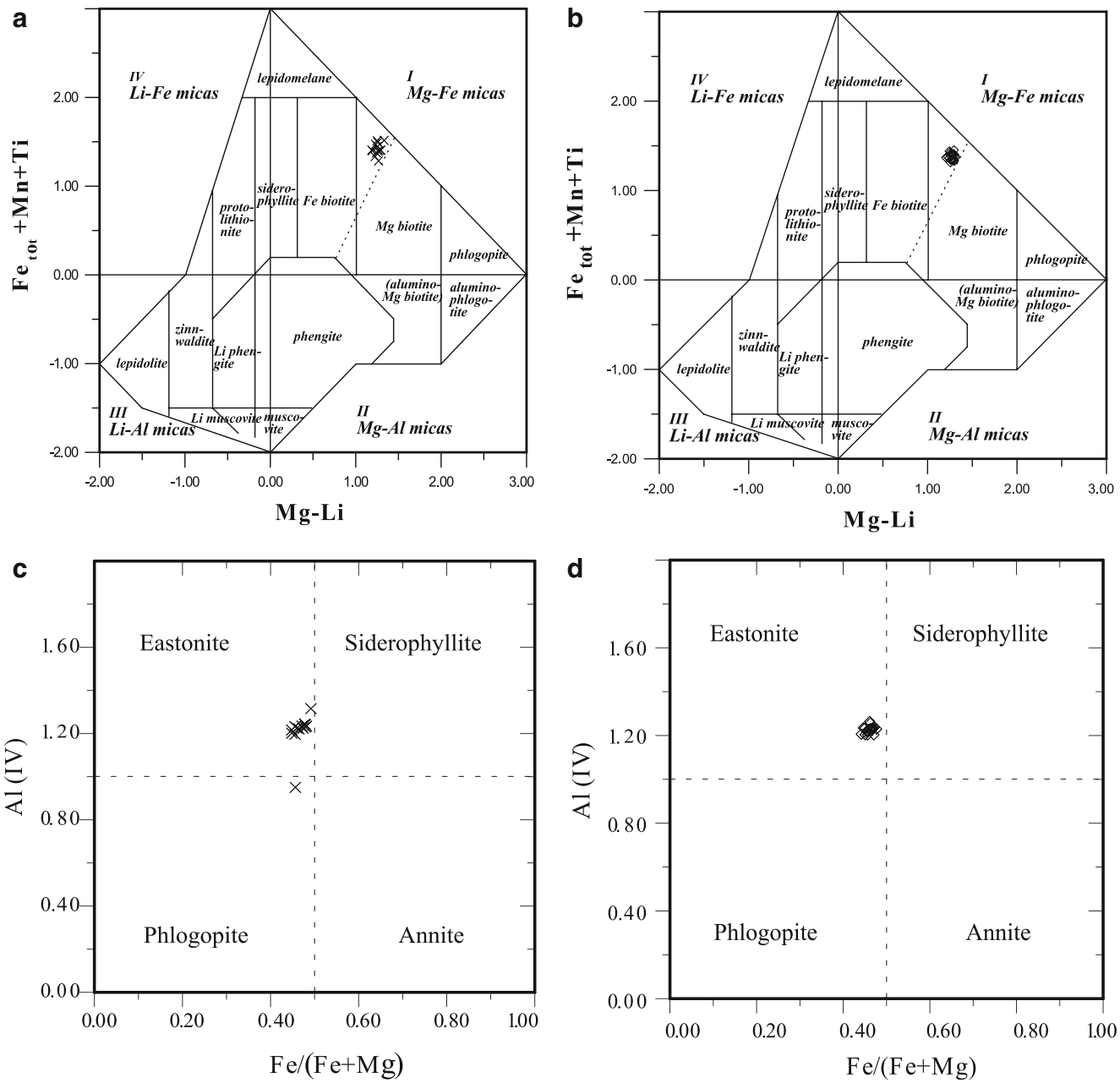

Fig. 8 Nomenclature and classification of the biotites from granodiorite (**a**, **c**) and their enclaves (**b**, **d**) (Foster 1960; Tischendorf et al. 1997)

Some chemical transfer could occur in place in the felsic host before the enclaves solidify (e.g., Frost and Mahood 1987; Vernon 1990; Wiebe 1994, 1996; Wiebe and Collins 1998), but the local ratio of mafic to felsic magma needs to be high enough to preserve the more mafic magma, which is sufficiently fluid for mixing to take place. In general, MMEs are too small and insulated for this process to take place, apart from possibly in the very margins of some enclaves. Consequently, the mixing typically takes place outside the present host magma chamber, most probably in deeper magma bodies that are disrupted upon encountering the main magma body, thus forming the MMEs that were scattered in the host magma.

As a geobarometer, the Al contents of calcic amphiboles can be used in plutonic rocks (Hammarstrom and Zen 1986; Hollister et al. 1987; Johnson and Rutherford 1989; Thomas and Ernst 1990; Schmidt 1992; Anderson and Smith 1995). The total pressure, fH_2O, and oxygen fugacity, in addition to the coexisting phases, influence the Al-content of hornblende. The tschermak substitution ($Si + R^{2+} = Al^{IV} + Al^{VI}$) is pressure sensitive (Hollister et al. 1987), while the edenite substitution ($Si + vac^{A} = Al^{IV} + (K + Na)^{A}$ and the reactions

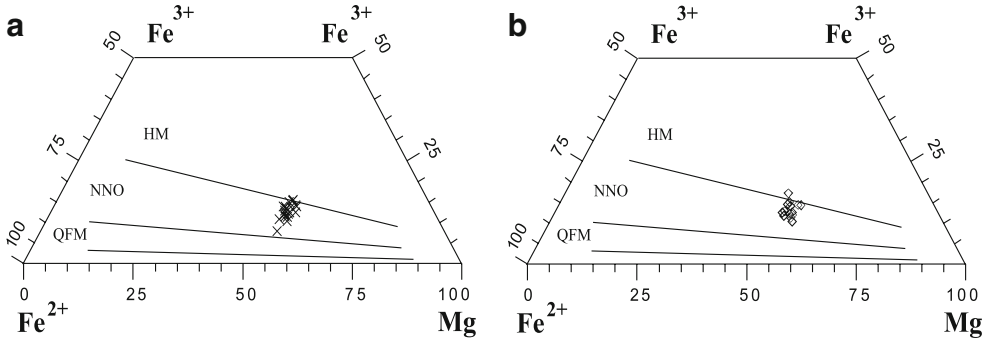

Fig. 9 Relationship of the Fe^{3+}-Fe^{2+}-Mg content of the biotites from granodiorite (**a**) and their enclaves (**b**) compared with buffered biotites from Wones and Eugster (1965)

involving Ti (e.g., $Ti + R^2 = 2Al^{VI}$ and $Ti + Al^{IV} = Al^{VI} + Si$) are temperature sensitive (Anderson and Smith 1995). The oxygen fugacity also plays a substantial role in the Al_{tot} content of the amphiboles. A high oxygen fugacity causes the insertion of Fe^{3+} into the lattice, which preferably substitutes Al, resulting in low Al-contents in the hornblende. Accordingly, it has been recommended that only amphiboles with a $Fe^{3+}/(Fe^{2+} + Fe^{3+})$-ratio ≥0:25 be used for barometric analyses (Anderson and Smith 1995). The amphiboles from the MMEs and granodiorites have a sufficiently appropriate chemical composition and can be used as good pressure indicators in igneous rocks. The method of Al-in-hornblende barometry of Anderson and Smith (1995) was utilised to infer the pressure at which the magma crystallised as it responded to the effect of temperature. The amphiboles from the enclaves and granodiorites yield a *P* of 0.7–4.1±0.6 kbar and 2.1–2.3±0.6 kbar at 730°C, respectively. Thus, magma mixing between mafic and felsic magmas took place possibly at some depth below the present exposure level during ascent from at least ~8 km (2.3 kbar). The discrepancy in pressure data for the enclaves may either reflect problems inherent to the Al-in-hornblende barometer or suggest that amphibole-melt equilibration may have occurred at levels deeper than that of the emplacement. The chemical composition of the secondary magnesiohornblendes (Si>7.3) were not used in the geobarometric calculations due to their low Al_{tot} contents, which induce too small (<0.5 kb) or too negative (e.g., −0.51 kb) pressure values.

Temperature data were calculated for the individual hornblende-plagioclase pairs of the different samples. A crystallisation temperature between 730 and 940±40°C for a pressure of 5 kbar was obtained from the amphibole–plagioclase geothermometer (Holland and Blundy 1994) in the MMEs. The temperature range estimated from thermometry is in accordance with experimental data on the liquidus temperature of the hornblende in granodiorites (<950 8C; Gilbert et al. 1982). In the geobarometer calculation, a temperature of 730°C was preferred, as it is lower than the interpreted peak magmatic temperatures within the hornblende stability field and because it eliminates both scatter and negative pressure estimates.

For the Horoz granitoids, the biotite chemistry of the samples suggests a calcalkaline orogenic setting. However, Kadioglu and Dilek (2009) suggest that Horoz granitoids have adakitic geochemical characteristics developed in the convergent margin and collisional tectonic settings. The samples could have been crystallised under moderately oxidising conditions, as evidenced by high Fe^{2+}/Fe^{3+} and

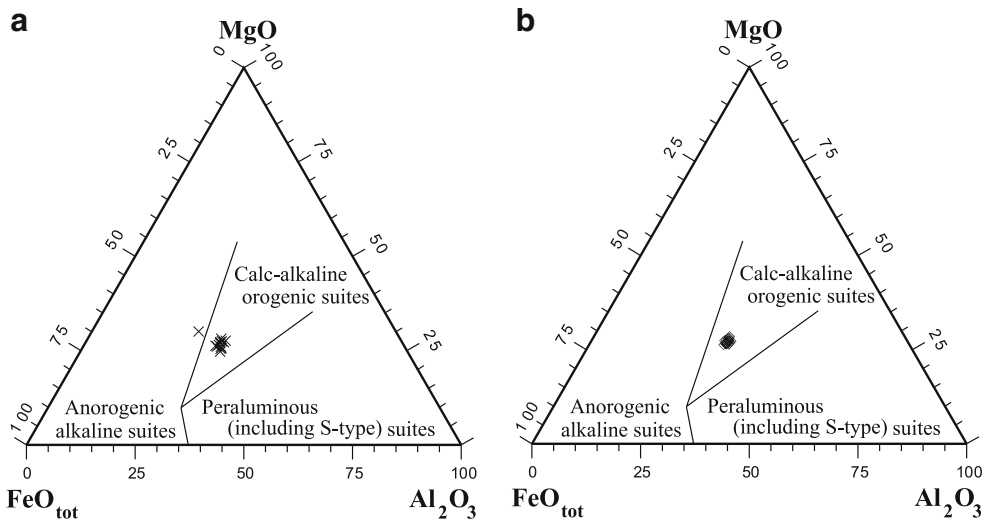

Fig. 10 Geotectonic setting of the biotites from granodiorite (**a**) and their enclaves (**b**) according to Abdel-Rahman (1994)

$[Fe^{3+}/(Fe^{3+} + Mg)]$ ratios in the biotite and amphibole, respectively. The extensive occurrence of amphibole and biotite as the main hydrous phases in the enclaves and their host supports the idea that these rocks, particularly mafic magma, have crystallised from a relatively water-rich magma. The existence of amphibole in a rock shows that the melt must have had a water content above some threshold value (the threshold level is controversial). Estimates of the amount of water needed to saturate a magma with amphibole range from a minimum of 6 wt.% (Merzbacher and Eggler 1984) to approximately 5% (Eggler 1972; Helz 1973; Naney 1983), and then to 2–3% (Luhr 1992). Therefore, the water content of the Horoz magma is possibly greater than 3%.

Two types of igneous enclaves have been determined in the calc-alkaline plutons of the CACC (Kadioglu and Gulec 1999; and Ilbeyli and Pearce 2005): (1) fine-grained to rarely porphyritic (Type-I); and (2) medium-grained to porphyritic with feldspar megacrysts (Type-II). Most common are the Type-I enclaves with quartz dioritic to quartz monzodioritic compositions and fine-grained margins. Less common are the Type-II enclaves, which have quartz dioritic to gabbro compositions and cumulate to porphyritic textures. The texture and mineralogy of the Horoz MMEs usually shows a similarity to that of Type-1 with quartz dioritic to quartz monzodioritic compositions, indicating an interaction between silicic magmas and mantle-derived melts.

Conclusions

The combination of field, textural and mineral chemical evidence leads to the conclusion that magma mixing and mingling of mafic basic to intermediate and felsic (granodiorite and granite) magmas played an important role in the petrogenesis of the adakitic Horoz intrusion. These plutons have textures that show significant magma mixing and mingling processes. Poikilitic, sieve and boxy cellular textures and inverse and oscillatory-zoned plagioclase with compositional spikes probably record the mixing of coexisting mafic and felsic magmas. The existence of acicular apatite and blade-like biotite also supports this suggestion. The textural and mineralogical evidence from the MMEs and host rocks demonstrates that magma mixing between the mafic and felsic magmas with high $f\,O_2$ took place at some depth below the present exposure level during its ascent from at least ~9 km and at more than 730°C. The identical mineral chemistry of biotite and plagioclase in the MMEs and their host suggest that these two minerals were possibly equilibrated. In comparison with the granodiorites, however, the higher content of Al, Ti, Fe^{2+}, Ca, Na and K and the lower content Si, Fe^{3+} and Mg in MMEs suggest that the MME hornblende is possibly of xenocrysts origin and was transferred from the MMEs into the felsic melt.

Acknowledgements This work was financially supported by the Office of Scientific Research (Bu calısma Selcuk Universitesi Bilimsel Arastırma Projeleri tarafından desteklenmistir. BAP; Project number: 5401041; Selcuk university; Turkey). The authors would like thank Bernard Barbarin and an anonymous reviewer for useful reviews of the manuscript and Associate Editor Ralf Milke for editorial handling.

References

Abdel-Rahman AFM (1994) Nature of biotites from alkaline, calc-alkaline and peraluminous magmas. J Petrol 35:525–541

Albuquerque CAR (1973) Geochemistry of biotites from granitic rocks, Northern Portugal. Geochim Cosmochim Acta 37:1779–1802

Anderson JL, Smith DR (1995) The effects of temperature and fO2 on the Al-in hornblende barometer. Am Mineral 80:549–559

Barbarin B (1990) Plagioclase xenocrysts and mafic magmatic enclaves in some granitoids of the Sierra Nevada batholith, California. J Geophys Res 95:17747–17756

Barbarin B (2005) Mafic magmatic enclaves and mafic rocks associated with some granitoids of the central Sierra Nevada batholith, California: nature, origin, and relations with the hosts. Lithos 80:155–177

Barbarin B, Didier J (1992) Genesis and evolution of mafic microgranular enclaves through various types of interaction between coexisting felsic and mafic magmas. Trans R Soc Edinb: Earth Sci 83:145–153

Barriere M, Cotten J (1979) Biotites and associated minerals as markers of magmatic fractionation and deuteric equilibration in granites. Contrib Mineral Petrol 70:183–192

Baxter S, Feely M (2002) Magma mixing and mingling textures in granitoids: examples from the Galway granite, Connemara, Ireland. Mineral Petrol 76:63–74

Beane RE (1974) Biotite stability in the porphyry copper environment. Econ Geol 69:241–256

Bingol E (1974) 1/2500,000 olcekli Turkiye metamorfizma haritası ve bazı metamorfik kusakların jeotektonik evrimi uzerine tartısmalar. MTA Enstitusu Dergisi 83:178–184 (in Turkish)

Blundy JD, Sparks RSJ (1992) Petrogenesis of mafic inclusions in granitoids of the Adamello Massif, Italy. J Petrol 33:1039–1104

Bonin B (2004) Do coeval mafic and felsic magmas in post-collisional to within-plate regimes necessarily imply two contrasting, mantle and crustal, sources? A review. Lithos 78:1–24

Çalapkulu F (1980) Geological study of Horoz Granodiorite. Bulletin of the Geological Society of Turkey 23:59–68 (Turkish with English abstract)

Çevikbaş A, Boztuğ D, Demirkol C et al (1995) Horoz plütonunun (Ulukışla- Niğde) oluşumunda dengelenmiş hibrid sistemin mineralojik ve jeokimyasal kanıtları. Türkiye Jeoloji Kurultayı Bülteni 10:62–77 (Turkish with English abstract)

Chappel BW, White AJR (1992) I- and S-types granites in the Lachland Fold Belt. Trans Royal Soc Edinb: Earth Sci 83:1–26

Chappell BW, White AJR, Wyborn D (1987) The importance of residual source material restite in granite petrogenesis. J Petrol 28:1111–1138

Chivas AR (1981) Geochemical evidence for magmatic fluids in porphyry copper mineralization. Contrib Mineral Petrol 78:389–403

Clark M, Robertson A (2002) The role of the early Tertiary Ulukisla Basin, southern Turkey, in suturing of the Mesozoic Tethys ocean. J Geol Soc London 159:673–690

Dahlquist JA (2002) Mafic microgranular enclaves: early segregation from metaluminous magma (Sierra de Chepes), Pampean Ranges, NW Argentina. J S Am Earth Sci 15(6):643–655

Didier J (1973) Granites and their enclaves. Elsevier, London, p 393

Didier J (1987) Contribution of enclave studies to the understanding of origin and evolution of granitic magmas. Geol Rundsch 79:41–50

Didier J, Barbarin B (1991) Enclaves and granite petrology, developments in petrology. Elsevier, Amsterdam, pp 1–625

Dilek Y, Whitney DL, Tekeli O (1999) Links between tectonic processes and landscape morphology in an Alpine collision zone, South-Central Turkey. Zeitschr Geomorph NF 118:147–164

Dodge FCW, Smith VC, Mays RE (1969) Biotites from granitic rocks of the Central Sierra Nevada Batholith, California. J Petrol 10:250–271

Dorais MJ, Whitney JA, Roden MF (1990) Origin ofmafic enclaves in the Dinkey Creek Pluton, Central Sierra Nevada batholith, California. J Petrol 31:853–881

Droop GTR (1987) A general equation for estimating Fe3+ concentrations in ferromagnesian silicates and oxides from microprobe analyses, using stochiometric criteria. Mineral Mag 51:431–435

Dymek RF (1983) Titanium, aluminum and interlayer cation substitutions in biotite from high-grade gneisses, West Greenland. Am Mineral 68(9–10):880–899

Eggler DH (1972) Water-saturated and undersaturated melting relations in a Paricutin andesite and an estimate of water content in the natural magma. Contrib Mineral Petrol 34:261–271

Eichelberger JC (1980) Vesiculation of mafic magma during replenishment of silicic magma reservoirs. Nature 288:446–450

Feeley TC, Wilson LF, Underwood SJ (2008) Distribution and compositions magmatic inclusions in the Mount Helen dome, Lassen volcanic center, California: insights into magma chamber processes. Lithos 106:173–189

Foster MD (1960) Interpretation of the composition of trioctahedral micas. U S Geol Surv Prof Pap 354-B:11–49

Frost TP, Mahood GA (1987) Field, chemical, and physical constraints on mafic–felsic magma interaction in the Lamarck granodiorite, Sierra Nevada, California. Geol Soc Am Bull 99:272–291

Gilbert MC, Helz RT, Popp RK, Spear FS (1982) Experimental studies of amphibole stability. In: Veblen DR, Ribbe PH (eds) Amphiboles: petrology and experimental phase relations. Rev Mineral 9B:229–353

Gorur N, Oktay F, Seymen I, Sengor AMC (1984) Paleotectonic evolution of the Tuzgolu basin complex, central Turkey: sedimentary record of a Neo-Tethyan closure In: Dixon JE, Robertson AHF (eds) The geological evolution of the Eastern Mediterranean. Geol Soc London, Spec Publ 17:467–482

Gorur N, Tuysuz O, Sengor AMC (1998) Tectonic evolution of the Central Anatolian basins. Int Geol Rev 40:831–850

Hammarstrom JM, Zen E (1986) Aluminium in hornblende: an empirical igneous geobarometer. Am Mineral 71:1297–1313

Helz RT (1973) Phase relations of basalts in their melting ranges at P_{H2O}=5 kb as a function of oxygen fugacity. J Petrol 14:249–302

Hendry DAF, Chivas AR, Long JVP, Reed SJB (1985) Chemical differences between minerals from mineralizing and barren intrusions from some North American porphyry copper deposits. Contrib Mineral Petrol 89:317–329

Hibbard MJ (1981) The magma mixing origin of mantled feldspars. Contrib Mineral Petrol 76:158–170

Hibbard MJ (1991) Textural anatomy of twelve magma-mixed granitoid systems. In: Didier J, Barbarin B (eds) Enclaves and granite petrology. Elsevier, Amsterdam, pp 431–444

Hibbard MJ (1995) Petrography to petrogenesis. Prentice Hall, New Jersey, pp 1–587

Hietanen A (1974) Amphibole pairs, epidote minerals, chlorite, and plagioclase in metamorphic rocks, northern Sierra Nevada, California. Am Mineral 59:22–40

Holland T, Blundy J (1994) Non-ideal interactions in calcic amphiboles and their bearing on amphibole-plagioclase thermometry. Contrib Mineral Petrol 116:433–447

Hollister LS, Grissom GC, Peters EK, Stowell HH, Sisson VB (1987) Confirmation of the empirical correlation of Al in hornblende with pressure of solidification of calc-alkaline plutons. Am Mineral 72:231–239

Ilbeyli N, Pearce JA (2005) Petrogenesis of igneous enclaves in plutonic rocks of the Central Anatolian Massif, Turkey. Intern Geol Rev 47:1011–1034

Jacobs DC, Parry WT (1979) Geochemistry of biotite in the Santa Rita Porphyry copper deposit, New Mexico. Econ Geol 74:860–887

Johnson MC, Rutherford MJ (1989) Experimental calibration of the aluminium-in hornblende geobarometer with applications to Long Valley caldera (California) volcanic rocks. Geology 17:837–841

Kadioglu YK, Dilek Y (2009) Structure and geochemistry of the adakitic Horoz granitoid, Bolkar Mountains, south-central Turkey, and its tectonomagmatic evolution. Intern Geol Rev 52:505–535

Kadioglu YK, Gulec N (1999) Types and genesis of the enclaves in central Anatolian granitoids. Geol J 34:243–256

Kaygusuz A, Aydıncakır E (2009) Mineralogy, whole-rock and Sr–Nd isotope geochemistry of mafic microgranular enclaves in Cretaceous Dagbasi granitoids, Eastern Pontides, NE Turkey: evidence of magma mixing, mingling and chemical equilibration. Chem Erde 69 (3):247–277

King BC (1964) The nature of basic igneous rocks and their relations with associated acid rocks. Sci Prog 52:282–292

Kocak K (2000) Horoz granodiyoritlerinin jeokimyası, N.Ü.Aksaray Müh. Fak., Jeoloji Müh Böl.&Sedimantaloji çalışma gurubu, Haymana-Tuzgölü-Ulukışla basenlerinin uygulamalı çalışması (workshop), 42

Kocak K (2006) Hybridization of mafic microgranular enclaves: mineral and whole-rock chemistry evidence from the Karamadazi Granitoid, Central Turkey. Intern J Earth Sci 95:587–607

Leake BE, Woolley AR, Arps CES et al (1997) Nomenclature of amphiboles: report of the subcomittee on amphiboles of the international mineralogical association, commission on new minerals and mineral names. Am Mineral 82:1019–1037

Luhr JF (1992) Slab-derived fluids and partial melting in subduction zones: insights from two contrasting Mexican volca noes _Colima and Ceboruco. J Volcanol Geotherm Res 54:1–18

Merzbacher C, Eggler DH (1984) A magmatic geohygrometer: application to Mount St. Helens and other dacitic magmas. Geology 12:587–590

Michael PJ (1991) Intrusion of basaltic magma into a crystallizing granitic magma chamber: the Cordillera del Paine pluton in southern Chile. Contrib Mineral Petrol 108:396–418

Naney MT (1983) Phase equilibria of rock-forming ferromagnesian silicates in granitic systems. Am J Sci 283:993–1033

Neiva AMR (1981) Geochemistry of hybrid granitoid rocks and of their biotites from Central Northern Portugal and their petrogenesis. Lithos 14:149–163

Nelson ST, Montana A (1992) Sieve-textured plagioclase in volcanic rocks produced by rapid decompression. Am Mineral 77:1242–1249

Noyes HJ, Frey FA, Wones DR (1983) A tale of two plutons: geochemical evidence bearing on the origin and differentiation of the Red Lake and Eagle Peak plutons, Central Sierra Nevada, California. J Geol 91:487–509

Parlak O, Karaoğlan F, Klötzli U, Koller F, Rizaoğlu T (2010) Geochronology of Turkish ophiolites: La-ICP-MS zircon U-Pb ages from the Inner Tauride and Bitlis-Zagros Suture Zones. 7th International Symposium on Eastern Mediterranean Geology, 18-20th October, Adana-Turkey

Perugini D, Poli G, Christofides G, Eleftheriadis G (2003) Magma mixing in the Sithonia plutonic complex, Greece: evidence from mafic microgranular enclaves. Mineral Petrol 78:173–200

Pringle GJ, Trembath LT, Parjari GE Jr (1974) Crystallization history of a zoned plagioclase. Mineral Mag 39:867–877

Qin JF, Lai SC, Diwu CR et al (2009) Magma mixing origin for the post-collisional adakitic monzogranitegranite of the Triassic Yangba pluton, Northwestern margin of the South China block: geochemistry, Sr–Nd isotopic, zircon U–Pb dating and Hf isotopic evidences. Contrib Mineral Petrol 159:389–409

Reid JB, Evans OC, Fates DG (1983) Magma mixing in granitic rocks of the central Sierra Nevada, California. Earth Planet Sci Lett 66:243–261

Rieder M (2001) Mineral nomenclature in the mica group: the promise and the reality. Eur J Mineral 13:1009–1012

Schmidt MW (1992) Amphibole composition in tonalite as a function of pressure: an experimental calibration of the Al-in- hornblende barometer. Contrib Mineral Petrol 110:304–310

Sengor AMC, Yilmaz Y (1981) Tethyan evolution of Turkey: a plate tectonic approach. Tectonophysics 75:181–241

Silva MMVG, Neiva AMR, Whitehouse MJ (2000) Geochemistry of enclaves and host granites from the Nelas area, central Portugal. Lithos 50:153–170

Sparks RSJ, Marshall A (1986) Thermal and mechanical constraints on mixing between mafic and silicic magmas. J Volc Geotherm Res 29:99–124

Stomer JC (1972) Mineralogy and Petrology of the Raton-Clayton volcanic field, northeastern New Mexico. Geol Soc Am Bull 83:3299–3322

Thomas WM, Ernst WG (1990) The aluminium content of hornblende in calc-alkaline granitic rocks: a mineralogic barometer calibrated experimentally to 12 kbar. In: Spencer RJ, Chou IM (eds) Fluid-mineral interactions: a tribute to HP Eugster. Geochem Soc Spec Publ 2:59–63

Tischendorf G, Gottesmann B, Förster HJ, Trumbull RB (1997) On Li-bearing micas: estimating Li from electron microprobe analyses and improved diagram for graphical representation. Mineral Mag 61:809–834

Tsuchiyama A (1985) Dissolution kinetics of plagioclase in melt of the system diopside-albite-anorthite and the origin of dusty plagioclase in andesites. Contrib Mineral Petrol 89:1–16

Vernon RH (1983) Restite, xenoliths and microgranitoid enclaves in granites. J Proc R Soc N S W 116:77–103

Vernon RH (1984) Microgranitoid enclaves: globules of hybrid magma quenched in a plutonic environment. Nature 304:438–439

Vernon RH (1990) Crystallization and hybridism in microgranitoid enclave magmas: microstructural evidence. J Geophys Res 95:17849–17859

Vernon RH (1991) Interpretation of microstructures of microgranitoid enclaves. In: Didier J, Barbarin B (Eds), Enclaves and Granite Petrology. Developments in Petrology, vol. 13. Elsevier, Amsterdam, pp. 277–291.

Vernon RH, Etheridge ME, Wall VJ (1988) Shape and microstructure of microgranitoid enclaves: indicators of magma mingling and flow. Lithos 22:1–11

Waight TE, Maas R, Nicholls IA (2001) Geochemical investigations of microgranitoid enclaves in the S-type Cowra Granodiorite, Lachlan Fold Belt, SE Australia. Lithos 56:165–186

Wall VJ, Clemens JD, Clarke DB (1987) Models for granitoid evolution and source compositions. J Geol 95:731–749

White RV, Tarney J, Kerr AC, Saunders AD, Kempton PD, Pringle MS, Klaver GT (1999) Modification of an oceanic plateau, Aruba, Dutch Caribbean: implications for the generation of continental crust. Lithos 46:43–68

Wiebe RA (1968) Plagioclase stratigraphy: a record of magmatic conditions and events in a granite stock. Am J Sci 266:690–703

Wiebe RA (1994) Silicic magma chambers as traps for basaltic magmas: the Cadillac Mountain Intrusive Complex, Mount Desert Island, Maine. J Geol 102:423–437

Wiebe RA (1996) Mafic–silicic layered intrusions; the role of basaltic injections on magmatic processes and the evolution of silicic magma chambers. In: Brown M, Candela PA, Peck DL, Stephens WE, Walker RJ, Zen E (eds) The Third Hutton Symposium on the Origin of Granites and Related Rocks. Geol Soc Am 315:233–242

Wiebe RA, Collins WJ (1998) Depositional features and stratigraphic sections in granitic plutons: implications for the emplacement and crystallization of granitic magma. J Struct Geol 20:1273–1289

Wiebe RA, Smith D, Sturn M, King EM (1997) Enclaves in the Cadillac mountain granite (Coastal Maine): samples of hybrid magma from the base of the chamber. J Petrol 38:393–426

Wones DR, Eugster HP (1965) Stability of biotite: experiment, theory, and application. Am Mineral 50:1228–1272

Wyllie PJ, Cox KG, Biggar GM (1962) The habit of apatite in synthetic systems and igneous rocks. J Petrol 3:238–243

Yang JH, Wu FY, Chung SL (2006) A hybrid origin for the Qianshan A-type granite, northeast China: geochemical and Sr–Nd–Hf isotopic evidence. Lithos 89:89–106

Yang JH, Fu-Yuan Wu FY, Wilde SA et al (2007) Tracing magma mixing in granite genesis: in situ U–Pb dating and Hf-isotope analysis of zircons. Contrib Mineral Petrol 153:177–190

Yavuz F (2003) Evaluating micas in petrologic and metallogenic aspect: Part II—Applications using the computer program Mica+. Comp Geosci 279:1215–1228